Molecular Cell
Short Article

Tissue-Specific Alternative Splicing Remodels Protein-Protein Interaction Networks

Jonathan D. Ellis,[1,5] Miriam Barrios-Rodiles,[2,5] Recep Çolak,[1,3,5] Manuel Irimia,[1] TaeHyung Kim,[1,3] John A. Calarco,[1,4,6] Xinchen Wang,[1,7] Qun Pan,[1] Dave O'Hanlon,[1] Philip M. Kim,[1,3,4,*] Jeffrey L. Wrana,[2,4,*] and Benjamin J. Blencowe[1,4,*]
[1]Banting and Best Department of Medical Research, Donnelly Centre, University of Toronto, Toronto, ON M5S 3E1, Canada
[2]Center for Systems Biology, Samuel Lunenfeld Research Institute, Mount Sinai Hospital, Toronto, ON M5G 1X5, Canada
[3]Department of Computer Science, University of Toronto, Toronto, ON M5S 2E4, Canada
[4]Department of Molecular Genetics, University of Toronto, Toronto, ON M5S 1A8, Canada
[5]These authors contributed equally to this work
[6]Present address: FAS Center for Systems Biology, Harvard University, Cambridge, MA 02138, USA
[7]Present address: Department of Biology, Massachusetts Institute of Technology, Cambridge, MA 02139, USA
*Correspondence: pm.kim@utoronto.ca (P.M.K.), wrana@lunenfeld.ca (J.L.W.), b.blencowe@utoronto.ca (B.J.B.)
DOI 10.1016/j.molcel.2012.05.037

SUMMARY

Alternative splicing plays a key role in the expansion of proteomic and regulatory complexity, yet the functions of the vast majority of differentially spliced exons are not known. In this study, we observe that brain and other tissue-regulated exons are significantly enriched in flexible regions of proteins that likely form conserved interaction surfaces. These proteins participate in significantly more interactions in protein-protein interaction (PPI) networks than other proteins. Using LUMIER, an automated PPI assay, we observe that approximately one-third of analyzed neural-regulated exons affect PPIs. Inclusion of these exons stimulated and repressed different partner interactions at comparable frequencies. This assay further revealed functions of individual exons, including a role for a neural-specific exon in promoting an interaction between Bridging Integrator 1 (Bin1)/Amphiphysin II and Dynamin 2 (Dnm2) that facilitates endocytosis. Collectively, our results provide evidence that regulated alternative exons frequently remodel interactions to establish tissue-dependent PPI networks.

INTRODUCTION

Alternative splicing (AS) affects transcripts from ~95% of multiexon human genes, and most of the resulting mRNA variants are variably expressed between human cell and tissue types (Pan et al., 2008; Wang et al., 2008). Specific subsets of alternative exons, or "exon networks," display coordinated regulation between different cell types or conditions (Calarco et al., 2011; Kalsotra and Cooper, 2011; Licatalosi and Darnell, 2010). Such exons are often evolutionarily conserved and enriched in genes with related functions, implying that they are involved in important processes or pathway-specific activities. To date, however, the functions of alternative exons within these networks have not been systematically investigated.

Analysis of splicing and protein tertiary structure has suggested that alternative exons can have diverse effects on protein folding and function (Birzele et al., 2008) but are also found on the surfaces, within loops or in predicted disordered regions of proteins (Romero et al., 2006; Wang et al., 2005). Since disordered regions are highly enriched in ligand binding surfaces and posttranslational modification, this suggests that AS may frequently modulate protein-protein and other ligand interactions (Dunker et al., 2008). Indeed, about 70% of proteins with exons that are regulated by the neural-specific splicing factor Nova form interactions with one another (Ule et al., 2005), and many of these exons overlap predicted phosphorylation sites (Zhang et al., 2010). In contrast, differentially regulated alternative exons have not been examined for common functional features. This is an important issue to address, since these exons are generally conserved and maintain frame. Moreover, because they comprise only 10%–30% of total alternative exons, they may possess important functional features that have been overlooked (Wang et al., 2008; Xing and Lee, 2005).

In this study, we systematically investigate properties of tissue-regulated alternative exons. We find that proteins containing these coding exons tend to have more interactions in PPI networks. Moreover, these exons, together with the flanking constitutive exons, are enriched in sequences predicted to be highly disordered. These properties are also found in proteins containing a brain-specific alternative exon network regulated by the nSR100/SRRM4 (neural-specific Ser/Arg-repeat related protein of 100 kDa), a recently identified AS regulator that is important for neuronal differentiation in vertebrates (Calarco et al., 2009; Raj et al., 2011). Using LUMIER, a high-throughput coimmunoprecipitation assay (Barrios-Rodiles et al., 2005), we observe that inclusion of nSR100-regulated exons can both promote and disrupt partner interactions, with a subset having very pronounced effects on PPIs. We show that one such exon, which promotes an interaction between Bin1/Amphiphysin II and the GTPase Dnm2, is important for efficient endocytosis

in neural cells. Collectively, our results support a widespread role for regulated alternative exons in controlling the tissue-specific dynamics of PPI networks.

RESULTS AND DISCUSSION

Global Network and Sequence Features of Proteins with Tissue-Dependent Alternative Exons

To investigate general functions of tissue-regulated exons, we asked if they are enriched in specific classes of proteins, protein domains, or regions. Human proteins containing coding sequences overlapping brain- or muscle-specific alternative exons were compared to proteins hosting "general" alternative coding exons, defined here as alternative exons that may or may not be tissue regulated (see the Supplemental Experimental Procedures for details). We analyzed "degree" and "betweenness" of these proteins; degree is the number of partners a protein has, and betweenness describes how central a protein is in a PPI network (Barabasi et al., 2011; Yu et al., 2007). Proteins with tissue-specific alternative exons have significantly higher degree and betweenness distributions than do proteins with general alternative exons (compare distributions of red and gray data points in Figures 1A and 1B; $p < 2.5e\text{-}10$ for degree and $p < 9.4e\text{-}10$ for betweenness, Wilcoxon rank sum test). Similar results were obtained when a comparable analysis was performed on mouse protein sets (see Figures S1A and S1B available online). Collectively, these results suggest that tissue-regulated alternative exons are important for the structure and function of PPI networks.

We next examined regulated AS events for features associated with PPIs. Alternative exons differentially included in brain, heart, and/or skeletal muscle, and the immediate flanking constitutive exons, contained significantly more residues predicted to be highly disordered than found in general alternative exons (Figure 1C, $p < 3.9\ e\text{-}13$, Wilcoxon rank sum test). Analysis of flanking constitutive exons when alternative exons are skipped, which can affect disorder rate due to context-dependent effects, yielded similar results (Figure 1D, $p < 9.60e\text{-}14$, Wilcoxon rank sum test). A comparable analysis performed on sets of mouse proteins also produced similar results (Figures S1C and S1D). In contrast, residues in distal constitutive exons of the same proteins did not display increased disorder rates compared to general alternative exons (Figure 1C; refer to legend and the Supplemental Information). Analysis of alternative exons differentially regulated in several other (but not all) tissues revealed similar results (Figure S1E).

Interestingly, tissue-regulated exons associated with the highest rates of disordered amino acids also tended to be the most highly conserved (Figure S1F and data not shown). For example, 63% of the 101 most disordered human brain, skeletal, and or heart-differentially spliced exons are also alternatively spliced in mouse, whereas only 31% of the least disordered 81 exons differentially spliced in these tissues were detected as alternatively spliced exons in mouse ($p < 0.0063$, one-tailed Fisher's exact test; refer to the Supplemental Information). Consistent with these and previous observations (Pan et al., 2004), tissue-regulated alternative coding exons and flanking constitutive exons less often overlapped folded protein domains compared to general alternative exons (Figures 1C; $p < 0.03$, Wilcoxon rank sum test). This depletion was most pronounced for highly disordered tissue-specific AS events compared to those with low or no disorder (Table S1). By contrast, eukaryotic linear motifs, which are often found within disordered regions and associated with PPIs (Davey et al., 2010; Weatheritt et al., 2012), were highly enriched within the tissue-specific AS events, particularly those containing highly disordered regions ($p = 2.3\ e\text{-}07$, Fisher's exact test; data not shown). Given these findings, we hypothesized that tissue-regulated alternative exons may play a widespread role in controlling PPIs.

Systematic Analysis of Neural Exons in Modulating PPIs

To systematically investigate the functions of tissue-regulated exons in PPIs, we employed luminescence-based mammalian interactome mapping (LUMIER) (Figure 2A) (Barrios-Rodiles et al., 2005), an automated coimmunoprecipitation assay in which "bait" cDNAs fused to *Renilla* luciferase (RL), and differing only by the presence or absence of a tissue-regulated alternative exon of interest, were coexpressed in HEK293T cells with triple Flag-tagged (3Flag) known or putative partner "prey" proteins. Coimmunoprecipitation of each RL bait with each 3Flag prey was measured semiquantitatively as normalized LUMIER intensity ratios (NLIRs) (Braun et al., 2009), which allowed us to assess whether inclusion of alternative exons affects PPI interactions.

We first performed a pilot screen employing bait proteins containing nine tissue-regulated exons (RAPGEF1, RAP1GDS1, RAP1GAP, RAPGEF6, RAPGEF4, RAP1B, GRB2, KIFAP3, SMURF2), several of which are associated with GTP signaling (Table S2A), together with eight preys mined from the literature and proteomics resources (Figure 2B). We also tested reciprocal interactions by exchanging the RL and 3Flag tags. Of the 74 tested interactions, 12 displayed consistent exon-dependent changes of 2-fold or higher in two or more experiments (Table S2B). In particular, a strong GRB2 self-interaction was abolished by deletion of an alternative exon that overlaps a central SH2 domain in this protein (Figures 2C and 2D), whereas the GRB2-RAPGEF1 interaction was unaffected (Figure 2C). GRB2 forms a homodimer via an interlaced interaction between its SH2 and SH3 domains (Maignan et al., 1995) that is important for signaling activity (McDonald et al., 2008). Moreover, GRB2 lacking the SH2 domain has dominant-negative activity that suppresses proliferative signals and promotes programmed cell death (Fath et al., 1994). Our results strongly suggest that AS regulation of the SH2 domain controls GRB2 dimer formation and signaling activity. This pilot screen also revealed that the brain-regulated alternative exons in RAP1GDS1 and RAP1B inhibit interactions with RHOA and RAP1GAP, respectively (Figure 2B). Collectively, these observations demonstrate that tissue-regulated AS can control PPIs and supports the efficacy of LUMIER screening for such events.

Systematic Functional Mapping of nSR100/SRRM4-Regulated Alternative Exons

We next systematically investigated the function of neural exons regulated by nSR100/SRRM4, which activates inclusion of ~11% of brain-specific exons, a subset of which target

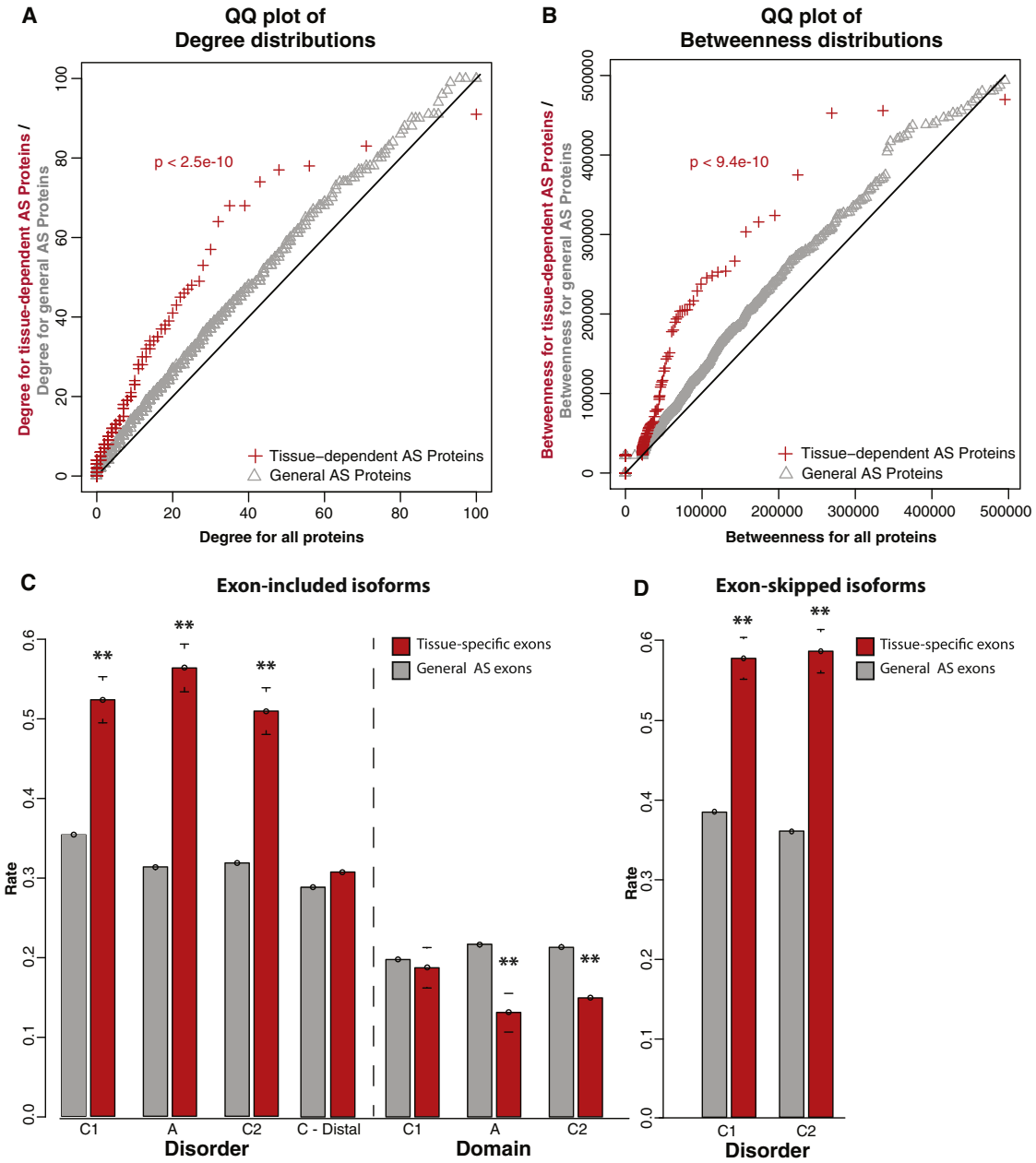

Figure 1. Network and Amino Acid Sequence Properties of Alternatively Spliced Proteins

(A) Quantile-Quantile (Q-Q) plot comparing distributions of "degree" (i.e., the number of times a protein forms interactions with other proteins) between proteins with tissue-dependent AS exons (red) and proteins with general AS exons (gray), versus all proteins. Tissue-dependent AS refers to cassette alternative exons differentially spliced between brain, skeletal muscle, and/or heart, relative to several other tissues (refer to the Supplemental Experimental Procedures).

(B) Q-Q plot comparing "betweenness" (the number of pairwise shortest paths between all pairs of nodes in a network that go through a protein, reflecting the extent of centrality or "hubness" of the protein) between proteins with tissue-dependent AS exons (red) and proteins with general AS exons (gray), versus all proteins. p values indicate statistically significant differences between the distributions of degree and betweenness values for proteins containing tissue-specific alternative exons and proteins containing general alternative exons (Wilcoxon rank sum test).

(C and D) Comparisons of the proportion of residues in specific coding exons that are intrinsically disordered or overlapping folded protein domains. Exon amino acid sequences from proteins containing general alternative exons (gray bars) are compared with exon amino acids from proteins containing tissue-dependent alternative exons (red bars). (C) compares properties of amino acid sequences for exon-included isoforms, whereas (D) compares properties of amino acid sequences for alternative exon-skipped isoforms. The percentage of amino acids within a specified exon predicted to be disordered was calculated and averaged across all exons for the set of proteins being compared. Protein disorder was derived using the software Disopred2 (Ward et al., 2004). Error bars indicate standard error. **p < 0.03, Wilcoxon rank sum test. A, alternative exon; C1, 5′ constitutive exon; C2, 3′ constitutive exon; C-Distal, constitutive exons that are separated from alternative exons by at least two constitutive exons.

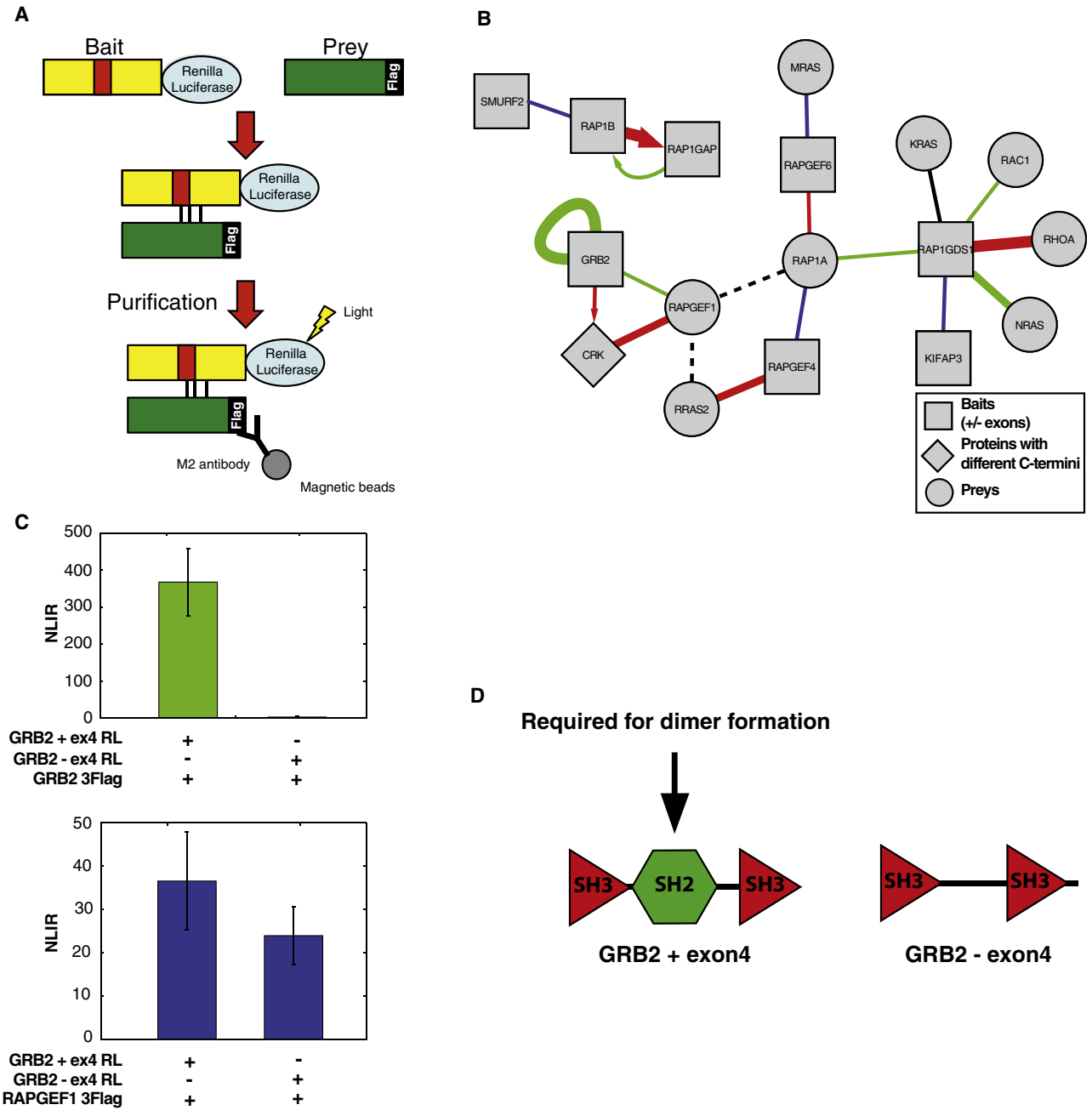

Figure 2. LUMIER Analysis of Effects of Alternative Exons on PPIs Involving GTP-Based Signaling Proteins

(A) Schematic of the LUMIER method used to determine whether an alternative exon (red box) regulates bait and prey interactions.

(B) Cytoscape diagram showing interactions tested by LUMIER in the pilot screen. Four experimental repeats were performed. For each bait (squares), a pair of cDNAs was constructed with the alternative exon included or skipped. Prey proteins are indicated by circles. CRK is shown as a diamond to indicate that proteins with different C termini were tested. Black edges represent tested interactions that were positive but not significantly affected by inclusion of an alternative exon; green edges represent interactions that were promoted by inclusion of an alternative exon; red edges represent interactions that were inhibited by inclusion of an alternative exon; blue edges represent tested interactions that were negative; dashed edges represent untested interactions. Arrows indicate the source of an alternative exon affecting a PPI interaction; for example, the alternative exon in RAP1B inhibited an interaction with RAP1GAP. The weight of the edge corresponds to the number of experimental repeats in which a 2-fold or greater change in NLIR value is observed upon inclusion or deletion of an alternative exon, with the weight being 1, 2, or 3.

(C) HEK293T cells were transfected with *Renilla* luciferase (RL)-tagged GRB2, with or without inclusion of the alternative exon 4, together with 3Flag-tagged GRB2 or RAPGEF1. NLIR values were calculated by measuring RL activity in immunoprecipitates recovered using anti-Flag antibody. Results shown are averages from four repeat experiments. Error bars show standard deviation.

(D) The domain diagram illustrates the requirement for the alternatively spliced SH2 domain for GRB2 dimerization.

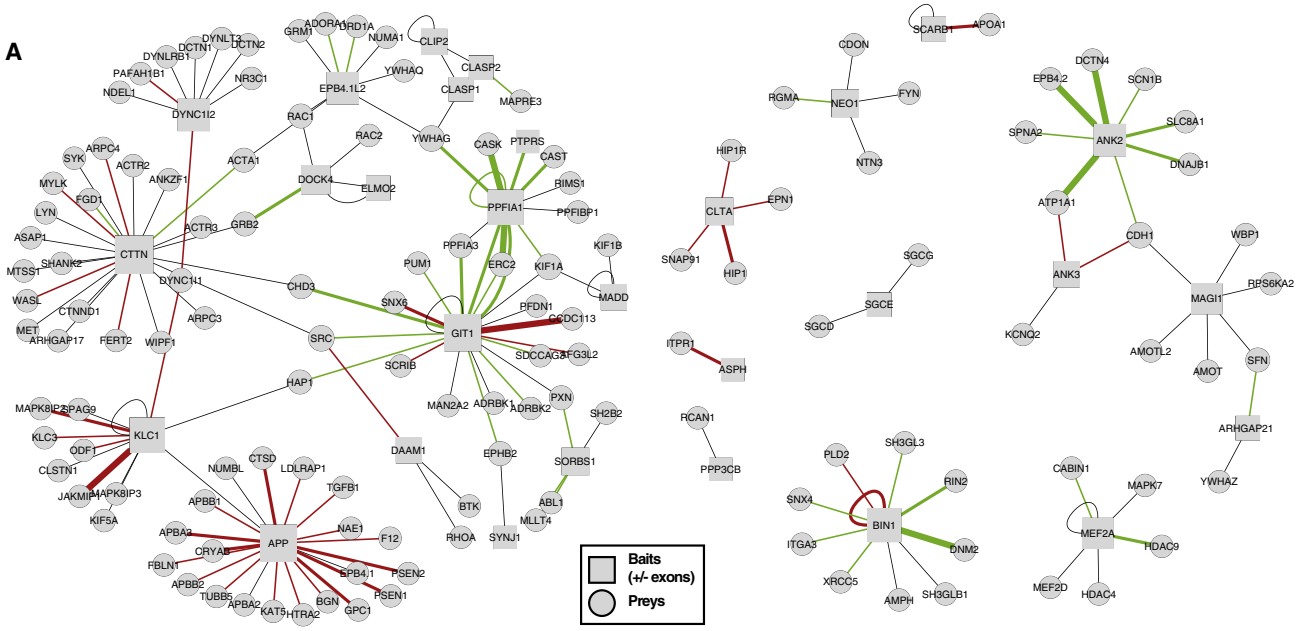
A
Baits
(+/- exons)
Preys

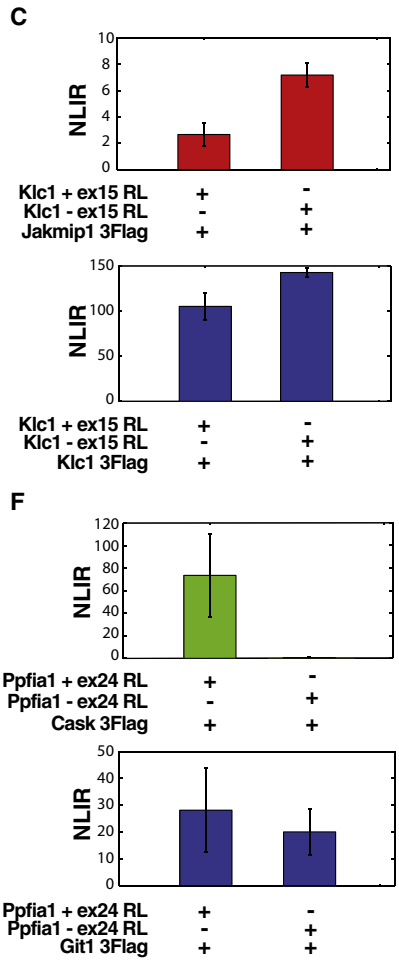
C
NLIR
Klc1 + ex15 RL
Klc1 - ex15 RL
Jakmip1 3Flag
NLIR
Klc1 + ex15 RL
Klc1 - ex15 RL
Klc1 3Flag
F
NLIR
Ppfia1 + ex24 RL
Ppfia1 - ex24 RL
Cask 3Flag
NLIR
Ppfia1 + ex24 RL
Ppfia1 - ex24 RL
Git1 3Flag

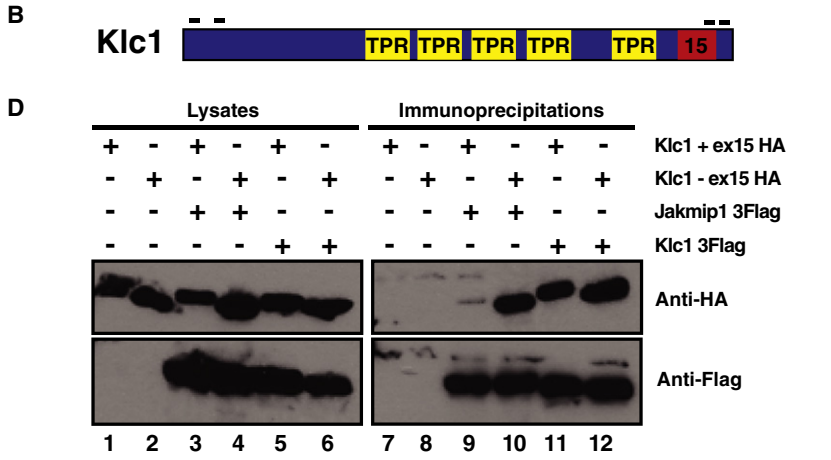
B
Klc1
TPR
TPR
TPR
TPR
TPR
15
D
Lysates
Immunoprecipitations
Klc1 + ex15 HA
Klc1 - ex15 HA
Jakmip1 3Flag
Klc1 3Flag
Anti-HA
Anti-Flag
1 2 3 4 5 6 7 8 9 10 11 12

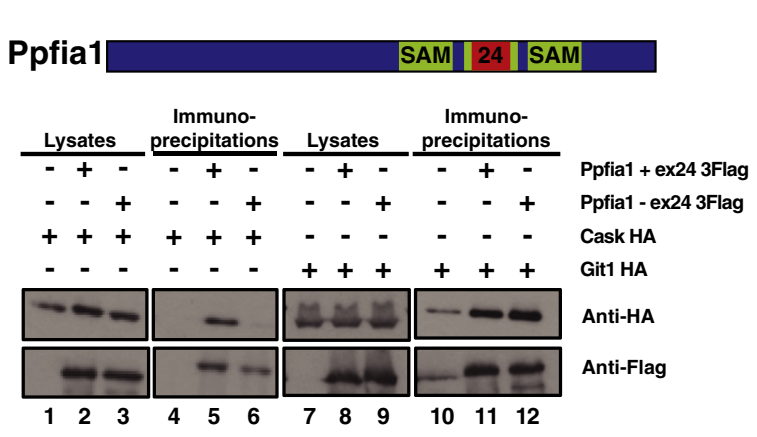
E
Ppfia1
SAM
24
SAM
G
Lysates
Immuno-
precipitations
Lysates
Immuno-
precipitations
Ppfia1 + ex24 3Flag
Ppfia1 - ex24 3Flag
Cask HA
Git1 HA
Anti-HA
Anti-Flag
1 2 3 4 5 6 7 8 9 10 11 12

cytoskeletal remodeling, membrane dynamics, or neuronal differentiation processes (Calarco et al., 2009; Raj et al., 2011). As found in the larger set of proteins with tissue-regulated exons (Figure 1 and Figure S1), proteins with nSR100 target exons display higher degree and betweenness distributions, and these exons are also enriched in regions of disorder (Figures S2B–S2E; p = 3.15e-5 for degree, p = 6.24e-5 for betweenness, and p = 5.7e-3 for disorder, Wilcoxon rank sum test).

Using LUMIER, we analyzed 31 mouse genes associated with "cytoskeletal organization and biogenesis," "synapse part," and "axon cargo transport" GO annotations that contain 34 nSR100-regulated coding alternative exons (Tables S3A and S3B). Of these exons, 83% are conserved, and all preserve frame when skipped or included (refer to the Supplemental Experimental Procedures). Interactions were tested among these and 355 additional known or putative partner proteins (Figure S2A and Supplemental Experimental Procedures) that lack nSR100-regulated exons, such that a total of 1,112 possible interactions were analyzed (Figure 3A). Following three rounds of LUMIER screening, 40.4% of tested interactions, involving at least one isoform, had an average NLIR $\geq$ 3.0 and were considered positive (Table S3C).

Remarkably, approximately one-third (10/34) of the exons affected one or more PPIs by at least 2-fold in at least two of the repeat screens (Table S3D and Figure 3A, edges weighted and colored to highlight interactions and exon-dependent changes). Seventy-six percent of these exon-dependent PPI changes occurred in the same direction; that is, inclusion of the exon resulted in either increased positive or increased negative PPI changes, but not both. This indicates that the majority of the exon-dependent interactions detected in the LUMIER screens are specific. Interestingly, despite the inclusion of nSR100 target exons potentially providing longer interaction interfaces, these exons promote or repress PPIs at comparable frequencies. Moreover, some of the nSR100-regulated exons (e.g., in Git1) can both promote and repress PPIs involving different partners, whereas other exons appear to only promote (e.g., in Ppfia1) or repress (e.g., in App) interactions. These observations suggest important, frequent, and highly specific roles for nSR100-regulated exons in controlling PPIs differentially between neural and nonneural cells.

Functional Characterization of Neural Exon-Dependent Regulation of PPIs

To confirm exon-dependent PPI changes detected in the LUMIER screens, coimmunoprecipitation western blot experiments were performed on a subset of interactions that changed by at least 2-fold (Figure 3, Figure 4, and Figures S2F–S2I; see below). These included exon-disrupting interactions involving Kinesin light chain (Klc1) or Amyloid beta (A4) precursor protein (App), and exon-promoting interactions involving Liprin alpha 1 (Ppfia1) or Bin1. Additional exon-modulated PPIs, and for comparison exon-independent PPIs, were also analyzed. This confirmed that inclusion of exon 15 in Klc1 disrupted an interaction with Janus kinase and microtubule-interacting protein 1 (Jakmip1/Marlin-1) with minimal effect on Klc1 self-interaction (Figures 3B–3D; lanes 9–12 in Figure 3D). A Jakmip1-Kinesin interaction in neurons links the cytoskeleton to gamma-aminobutyric acid B receptors (GABA[B]Rs) (Vidal et al., 2007), which are G protein-coupled receptors that control the slow component of inhibitory neurotransmission (Bettler et al., 2004). Our results thus suggest that nSR100-dependent AS of exon 15 in Klc1 might control GABA(B)Rs distribution and neurotransmission.

We also confirmed that exon 24 in the Liprin Ppfia1 strongly promotes an interaction with Calcium/calmodulin serine protein kinase (Cask) (Figures 3E–3G; compare lanes 5 and 6 in Figure 3G), while not affecting an interaction with Git1 (compare lanes 11 and 12 in Figure 3G). Liprins are scaffold proteins that regulate cell adhesion, cell migration, and synapse formation (Serra-Pages et al., 1998), and Ppfia1 is a cargo receptor that delivers Cask, a presynaptic scaffolding protein, to the developing synapse (Olsen et al., 2005; Shin et al., 2003). A cocrystal structure shows that the three sterile alpha motif (SAM) domains in Ppfia1 mediate Cask binding (Wei et al., 2011). Indeed, exon 24 overlaps one of these SAM domains (Figure 3E), whereas nSR100-regulated exon 17, which was also tested by LUMIER, does not overlap a SAM domain and did not affect the Cask

Figure 3. LUMIER Analysis of the Role of nSR100-Regulated Exons in Mediating PPIs

(A) Cytoscape visualization of PPIs analyzed by LUMIER. The diagram shows a subset of the entire modeled PPI network analyzed by LUMIER (refer to Figure S2), focusing on positive interactions. Three experimental repeats were performed. For each bait (squares), pairs of cDNAs were constructed with or without the inclusion of an nSR100-regulated alternative exon, and prey proteins are indicated by circles. As in Figure 2A, black edges represent positive but unaffected interactions; green edges represent interactions that were promoted by exon inclusion; red edges represent interactions that were inhibited by exon inclusion. Edges are weighted (1, 2, or 3) to indicate the number of repeat assays in which a 2-fold or greater change in NLIR value was observed when an alternative exon is included.

(B) Domain diagram for Klc1 illustrating the location of five tetratricopeptide repeat (TPR) domains in relation to exon 15 (red box), which overlaps a highly disordered region in the protein (indicated by a line).

(C) Quantification of LUMIER NLIR values for RL-tagged Klc1, with or without inclusion of exon 15, coimmunoprecipitated with Flag-tagged Jakmip1 or Flag-tagged Klc1. NLIR values are averaged from three repeat LUMIER experiments, and standard deviations are indicated.

(D) HEK293T cells were transfected with hemagglutinin (HA)- or 3Flag-tagged Klc1-expressing constructs, with or without inclusion of exon 15, together with 3Flag-tagged Jakmip1. Immunoprecipitation was performed with anti-Flag antibody, and the immunoprecipitates were blotted with anti-HA antibody (upper panels) and, to control for recovery, anti-Flag antibody (lower panels).

(E) Domain diagram for Ppfia1 shows the position of three sterile alpha motif (SAM) domains. Exon 24 (red box) is located within the second SAM domain.

(F) Quantification of LUMIER NLIR values for RL-tagged Ppfia1, with or without exon 24, coimmunoprecipitated with 3Flag-tagged Cask or Git1. NLIR values are averaged from the three repeat LUMIER experiments, and standard deviations are indicated.

(G) Neuro2a cells were transfected HA-tagged Cask or Git1 constructs, together with 3Flag-tagged Ppfia1, with or without exon 24, as indicated. Immunoprecipitation was performed with anti-Flag antibody, and the immunoprecipitates were blotted with anti-HA antibody (upper panels) and, to control for recovery, anti-Flag antibody (lower panels).

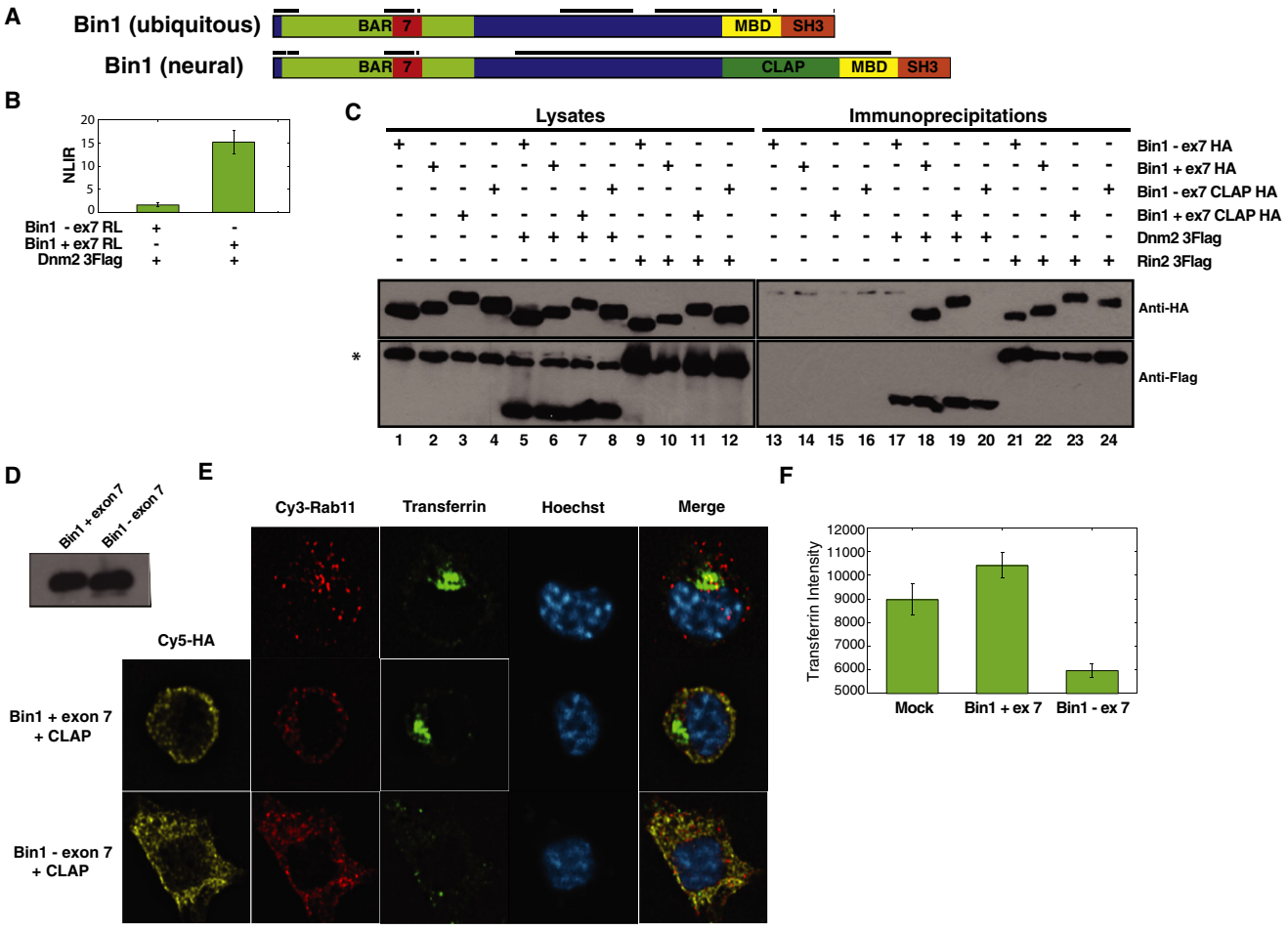

Figure 4. The nSR100-Regulated Exon 7 in Bin1 Promotes an Interaction with Dnm2 and Endocytosis

(A) Domain diagrams for ubiquitous and neural expressed isoforms of Bin1, illustrating the location of the nSR100-regulated exon 7 (red), in relation to Bin/Amphiphysin/Rvs (BAR) domain, Myc binding domain (MBD), Src homology-3 (SH3), and clathrin-AP2 binding (CLAP) domains in these isoforms. The line above the diagram indicates highly disordered regions (see also Figure S1E). The ubiquitous isoform was used in the LUMIER screens. This and the neural isoform containing the CLAP domain were used for coimmunoprecipitation western blotting experiments. The latter isoform, with or without exon 7, was used in endocytosis assays (see below).

(B) HEK293T cells were transfected with RL-tagged Bin1, with or without inclusion of the nSR100-regulated exon 7, together with Flag-tagged Dnm2. NLIR values were averaged over three repeat LUMIER experiments, and standard deviations are indicated.

(C) HEK293T cells were transfected with 3Flag-tagged Dnm2 or Rin2, together with HA-tagged Bin1, with or without exon 7, as indicated. Immunoprecipitation was performed with anti-Flag antibody, and the immunoprecipitates were blotted with anti-HA antibody (upper panels) and, to control for recovery, anti-Flag antibody (lower panels). CLAP, Clathrin/AP2 binding region.

(D) Neuro2a cells to be used for endocytosis assays (refer to E and F) were transfected with HA-tagged cDNA expression vectors expressing the CLAP domain-containing (neural) isoforms of Bin1, with or without exon 7 included. Lysates were collected, and equal amounts were separated by SDS-PAGE and immunoblotted with anti-HA antibody. Asterisk denotes a nonspecific band in lanes 1–8.

(E) Representative images are shown for uptake of transferrin coupled to Alexa Fluor 488 in Neuro2a cells, following transfection of expression vectors for Bin1 isoforms with or without exon 7 included, as analyzed in (D). Prior to confocal imaging, cells were incubated at 4°C for 2 hr with transferrin-Alexa Fluor 488 and then incubated at 37°C for 20 min. Cy5 channel shows HA staining; Cy3 channel shows anti-Rab11 immunostaining; GFP detection shows transferrin-Alexa Fluor 488 uptake.

(F) Volocity software analysis was used to quantify internalization of transferrin using a large pinhole to measure mean GFP intensities in recycling endosomes that are immunostained with an antibody specific for the recycling endosome marker, Rab11. Fifty cells were analyzed for each transfection condition indicated. Error bars show standard error.

interaction (Table S2C). Our results therefore suggest that nSR100-dependent Ppfia1 exon 24 inclusion might control Ppfia1 targeting of Cask to the developing synapse.

Finally, we examined Bin1/Amphiphysin II, which contains a Bin-Amphiphysin-Rvs (BAR) domain (Figure 4A and Figure S3), which binds curved regions of membranes (Peter et al., 2004). In synapses, Bin1 functions as an adaptor protein that heterodimerizes with Amphiphysin to facilitate endocytic uptake at highly curved clathrin-coated pits, via interactions with Dnm2, a large GTPase that mediates membrane fission by constricting

vesicle necks (Sever, 2002; Wigge et al., 1997). LUMIER revealed that nSR100-regulated exon 7, which overlaps a disordered region in the BAR domain, strongly promotes an interaction with Dnm2 but does not affect a Rin2 interaction (Figure 4B and Table S2C; see below). We confirmed that exon 7 promotes an interaction between Dnm2 and two isoforms of Bin1. One of these is ubiquitous and the other is neurally expressed and contains a Clathrin/AP2 binding (CLAP) domain (Figures 4A and 4C; compare lanes 17 and 20 with lanes 18 and 19 in Figure 4C) (Tsutsui et al., 1997). In contrast, exon 7 had little effect on the interaction with Rin2 (compare lanes 21 and 24 in Figure 4C).

We next investigated whether the exon 7-dependent interaction of Bin1 with Dnm2 might modulate the efficiency of endocytosis in neural cells. For this, we used Neuro2A cells transiently expressing neural isoforms of Bin1 including or lacking exon 7 and quantified uptake of Alexa Fluor 488-conjugated Transferrin into vesicles costained with the recycling endosome marker Rab11. Inclusion of exon 7 did not affect Bin1 protein levels (Figure 4D) but did result in a significant increase in transferrin uptake (Figures 4E and 4F, $p = 0.025$, Wilcoxon rank sum test). In contrast, overexpression of Bin1 lacking exon 7 inhibited transferrin uptake (Figure 4F; $p = 0.002$, Wilcoxon rank sum test). Since the Bin1 isoform lacking exon 7 can homodimerize and heterodimerize with Amphiphysin, its expression may sequester endogenous exon 7-containing Bin1 and Amphiphysin, thus preventing functional interactions with Dnm2. Collectively, our results suggest that the nSR100-regulated exon 7 of Bin1, by strongly promoting interaction with Dnm2, is important for efficient endocytosis in neural cells.

Conclusions

In this study, we present a systematic analysis of the function of AS events comprising a tissue-regulated exon network. We observe that approximately one-third of analyzed cassette exons regulated by the neural-specific splicing regulator nSR100 positively or negatively affect PPIs with one or more partners. This observation supports a widespread role for tissue-regulated AS events in the regulation of PPIs. The detected exon-dependent PPI changes may underrepresent the total number of AS-regulated PPI changes involving the same set of proteins, since additional partners for these proteins exist that were not tested and because the false-negative detection rate of LUMIER is estimated to be higher than its false-positive rate (Braun et al., 2009). Regardless, our results demonstrate that the systematic screening of alternative coding exons for modulation of PPIs provides a valuable approach for uncovering gene functions at an exon-level resolution. This is further exemplified by the follow-up analysis suggesting a functional role for Bin1 exon 7 in controlling the efficiency of neural cell endocytosis through its promotion of Dnm2 interactions.

EXPERIMENTAL PROCEDURES

Renilla Luciferase-Tagged and 3Flag-Tagged cDNAs

Gateway recombination cloning technology (Life Technologies) was used to generate C-terminal tagged RL cDNA "bait" clones containing or lacking alternative exons of interest, as well as C-terminal 3Flag-tagged cDNA "prey" clones. Details are provided in the Supplemental Information.

LUMIER Screens

LUMIER screens were carried out in HEK293T cells essentially as previously described (Barrios-Rodiles et al., 2005). Positive interactions had an NLIR of ≥ 3. Details of the screens and data analysis are provided in the Supplemental Experimental Procedures.

Immunoprecipitation

HEK293T cells were transiently transfected using Lipofectamine 2000 (Life Technologies). Cells were lysed in 0.5% TNTE (50 mM Tris [pH 7.4], 150 mM sodium chloride, 1 mM EDTA, 0.5% Triton X-100), and immunoprecipitations were carried out using specified antibodies. Refer to the Supplemental Experimental Procedures for details.

Endocytosis Assays

Neuro2a cells were transiently transfected using Lipofectamine 2000 (Life Technologies). Cells were chilled in cold serum-free media and then incubated with Alexa Fluor 488-conjugated transferrin (10 μg/ml, Life Technologies) in cold serum-free media for 2 hr at 4°C. Cells were washed with cold, serum-free medium to remove excess transferrin and then incubated in serum-containing media prewarmed to 37°C for 20 min. Cells were fixed in 4% paraformaldehyde in PBS and then processed for immunofluorescence. Refer to the Supplemental Experimental Procedures for details.

SUPPLEMENTAL INFORMATION

Supplemental Information includes three figures, three tables, Supplemental Experimental Procedures, and Supplemental References and can be found with this article online at doi:10.1016/j.molcel.2012.05.037.

ACKNOWLEDGMENTS

The authors are grateful to Daniel Tong for assistance with cDNA cloning, to Marina Olhovsky and Dr. Karen Colwill for cDNA clones (http://openfreezer.lunenfeld.ca/), to Thomas Sun and Drs. Frederick S. Vizeacoumar and Alessandro Datti for robotics screening (SMART collaborative center; http://robotics.lunenfeld.ca/), and to Drs. John DiGuglielmo and Masahiro Narimatsu for advice on transferrin uptake assays and confocal imaging. This research was supported by Canadian Institutes of Health Research Operating Grants (to B.J.B. and J.L.W.) and in part by a grant from the Ontario Research Fund to J.L.W., B.J.B., and others. M.I. is the recipient of a Human Frontiers Science Program Long-Term Fellowship.

Received: January 27, 2012
Revised: March 29, 2012
Accepted: May 7, 2012
Published online: June 28, 2012

REFERENCES

Barabasi, A.L., Gulbahce, N., and Loscalzo, J. (2011). Network medicine: a network-based approach to human disease. Nat. Rev. Genet. *12*, 56–68.

Barrios-Rodiles, M., Brown, K.R., Ozdamar, B., Bose, R., Liu, Z., Donovan, R.S., Shinjo, F., Liu, Y., Dembowy, J., Taylor, I.W., et al. (2005). High-throughput mapping of a dynamic signaling network in mammalian cells. Science *307*, 1621–1625.

Bettler, B., Kaupmann, K., Mosbacher, J., and Gassmann, M. (2004). Molecular structure and physiological functions of GABA(B) receptors. Physiol. Rev. *84*, 835–867.

Birzele, F., Csaba, G., and Zimmer, R. (2008). Alternative splicing and protein structure evolution. Nucleic Acids Res. *36*, 550–558.

Braun, P., Tasan, M., Dreze, M., Barrios-Rodiles, M., Lemmens, I., Yu, H., Sahalie, J.M., Murray, R.R., Roncari, L., de Smet, A.S., et al. (2009). An

experimentally derived confidence score for binary protein-protein interactions. Nat. Methods *6*, 91–97.

Calarco, J.A., Superina, S., O'Hanlon, D., Gabut, M., Raj, B., Pan, Q., Skalska, U., Clarke, L., Gelinas, D., van der Kooy, D., et al. (2009). Regulation of vertebrate nervous system alternative splicing and development by an SR-related protein. Cell *138*, 898–910.

Calarco, J.A., Zhen, M., and Blencowe, B.J. (2011). Networking in a global world: establishing functional connections between neural splicing regulators and their target transcripts. RNA *17*, 775–791.

Davey, N.E., Haslam, N.J., Shields, D.C., and Edwards, R.J. (2010). SLiMFinder: a web server to find novel, significantly over-represented, short protein motifs. Nucleic Acids Res. *38*, W534–W539.

Dunker, A.K., Silman, I., Uversky, V.N., and Sussman, J.L. (2008). Function and structure of inherently disordered proteins. Curr. Opin. Struct. Biol. *18*, 756–764.

Fath, I., Schweighoffer, F., Rey, I., Multon, M.C., Boiziau, J., Duchesne, M., and Tocque, B. (1994). Cloning of a Grb2 isoform with apoptotic properties. Science *264*, 971–974.

Kalsotra, A., and Cooper, T.A. (2011). Functional consequences of developmentally regulated alternative splicing. Nat. Rev. Genet. *12*, 715–729.

Licatalosi, D.D., and Darnell, R.B. (2010). RNA processing and its regulation: global insights into biological networks. Nat. Rev. Genet. *11*, 75–87.

Maignan, S., Guilloteau, J.P., Fromage, N., Arnoux, B., Becquart, J., and Ducruix, A. (1995). Crystal structure of the mammalian Grb2 adaptor. Science *268*, 291–293.

McDonald, C.B., Seldeen, K.L., Deegan, B.J., Lewis, M.S., and Farooq, A. (2008). Grb2 adaptor undergoes conformational change upon dimerization. Arch. Biochem. Biophys. *475*, 25–35.

Olsen, O., Moore, K.A., Fukata, M., Kazuta, T., Trinidad, J.C., Kauer, F.W., Streuli, M., Misawa, H., Burlingame, A.L., Nicoll, R.A., et al. (2005). Neurotransmitter release regulated by a MALS-liprin-alpha presynaptic complex. J. Cell Biol. *170*, 1127–1134.

Pan, Q., Shai, O., Misquitta, C., Zhang, W., Saltzman, A.L., Mohammad, N., Babak, T., Siu, H., Hughes, T.R., Morris, Q.D., et al. (2004). Revealing global regulatory features of mammalian alternative splicing using a quantitative microarray platform. Mol. Cell *16*, 929–941.

Pan, Q., Shai, O., Lee, L.J., Frey, B.J., and Blencowe, B.J. (2008). Deep surveying of alternative splicing complexity in the human transcriptome by high-throughput sequencing. Nat. Genet. *40*, 1413–1415.

Peter, B.J., Kent, H.M., Mills, I.G., Vallis, Y., Butler, P.J., Evans, P.R., and McMahon, H.T. (2004). BAR domains as sensors of membrane curvature: the amphiphysin BAR structure. Science *303*, 495–499.

Raj, B., O'Hanlon, D., Vessey, J.P., Pan, Q., Ray, D., Buckley, N.J., Miller, F.D., and Blencowe, B.J. (2011). Cross-regulation between an alternative splicing activator and a transcription repressor controls neurogenesis. Mol. Cell *43*, 843–850.

Romero, P.R., Zaidi, S., Fang, Y.Y., Uversky, V.N., Radivojac, P., Oldfield, C.J., Cortese, M.S., Sickmeier, M., LeGall, T., Obradovic, Z., et al. (2006). Alternative splicing in concert with protein intrinsic disorder enables increased functional diversity in multicellular organisms. Proc. Natl. Acad. Sci. USA *103*, 8390–8395.

Serra-Pages, C., Medley, Q.G., Tang, M., Hart, A., and Streuli, M. (1998). Liprins, a family of LAR transmembrane protein-tyrosine phosphatase-interacting proteins. J. Biol. Chem. *273*, 15611–15620.

Sever, S. (2002). Dynamin and endocytosis. Curr. Opin. Cell Biol. *14*, 463–467.

Shin, H., Wyszynski, M., Huh, K.H., Valtschanoff, J.G., Lee, J.R., Ko, J., Streuli, M., Weinberg, R.J., Sheng, M., and Kim, E. (2003). Association of the kinesin motor KIF1A with the multimodular protein liprin-alpha. J. Biol. Chem. *278*, 11393–11401.

Tsutsui, K., Maeda, Y., Seki, S., and Tokunaga, A. (1997). cDNA cloning of a novel amphiphysin isoform and tissue-specific expression of its multiple splice variants. Biochem. Biophys. Res. Commun. *236*, 178–183.

Ule, J., Ule, A., Spencer, J., Williams, A., Hu, J.S., Cline, M., Wang, H., Clark, T., Fraser, C., Ruggiu, M., et al. (2005). Nova regulates brain-specific splicing to shape the synapse. Nat. Genet. *37*, 844–852.

Vidal, R.L., Ramirez, O.A., Sandoval, L., Koenig-Robert, R., Hartel, S., and Couve, A. (2007). Marlin-1 and conventional kinesin link GABAB receptors to the cytoskeleton and regulate receptor transport. Mol. Cell. Neurosci. *35*, 501–512.

Wang, P., Yan, B., Guo, J.T., Hicks, C., and Xu, Y. (2005). Structural genomics analysis of alternative splicing and application to isoform structure modeling. Proc. Natl. Acad. Sci. USA *102*, 18920–18925.

Wang, E.T., Sandberg, R., Luo, S., Khrebtukova, I., Zhang, L., Mayr, C., Kingsmore, S.F., Schroth, G.P., and Burge, C.B. (2008). Alternative isoform regulation in human tissue transcriptomes. Nature *456*, 470–476.

Ward, J.J., Sodhi, J.S., McGuffin, L.J., Buxton, B.F., and Jones, D.T. (2004). Prediction and functional analysis of native disorder in proteins from the three kingdoms of life. J. Mol. Biol. *337*, 635–645.

Weatheritt, R., Luck, K., Petsalaki, E., Davey, N., and Gibson, T. (2012). The identification of short linear motif-mediated interfaces within the human interactome. Bioinformatics *28*, 976–982.

Wei, Z., Zheng, S., Spangler, S.A., Yu, C., Hoogenraad, C.C., and Zhang, M. (2011). Liprin-mediated large signaling complex organization revealed by the liprin-alpha/CASK and liprin-alpha/liprin-beta complex structures. Mol. Cell *43*, 586–598.

Wigge, P., Kohler, K., Vallis, Y., Doyle, C.A., Owen, D., Hunt, S.P., and McMahon, H.T. (1997). Amphiphysin heterodimers: potential role in clathrin-mediated endocytosis. Mol. Biol. Cell *8*, 2003–2015.

Xing, Y., and Lee, C.J. (2005). Protein modularity of alternatively spliced exons is associated with tissue-specific regulation of alternative splicing. PLoS Genet. *1*, e34. 10.1371/journal.pgen.0010034.

Yu, H., Kim, P.M., Sprecher, E., Trifonov, V., and Gerstein, M. (2007). The importance of bottlenecks in protein networks: correlation with gene essentiality and expression dynamics. PLoS Comput. Biol. *3*, e59. 10.1371/journal.pgen.0010034.

Zhang, C., Frias, M.A., Mele, A., Ruggiu, M., Eom, T., Marney, C.B., Wang, H., Licatalosi, D.D., Fak, J.J., and Darnell, R.B. (2010). Integrative modeling defines the nova splicing-regulatory network and its combinatorial controls. Science *329*, 439–443.